Received: 4 May 2023 | Revised: 10 July 2023 | Accepted: 11 July 2023

DOI: 10.1002/pol.20230282

RESEARCH ARTICLE

JOURNAL OF POLYMER SCIENCE WILEY

Engineering antimicrobial supramolecular polymer assemblies

Jiankang Song[1,2,3] | **Moniek G. J. Schmitz**[3] | **Martijn Riool**[4,5] | **Shuaiqi Guo**[1] | **Sebastian A. J. Zaat**[4] | **Patricia Y. W. Dankers**[1,2,3]

[1]Institute for Complex Molecular Systems, Eindhoven University of Technology, Eindhoven, Netherlands

[2]Department of Biomedical Engineering, Laboratory for Cell and Tissue Engineering, Eindhoven University of Technology, Eindhoven, Netherlands

[3]Department of Biomedical Engineering, Laboratory for Chemical Biology, Eindhoven University of Technology, Eindhoven, Netherlands

[4]Department of Medical Microbiology and Infection Prevention, Amsterdam institute for Infection and Immunity, Amsterdam UMC, University of Amsterdam, Amsterdam, Netherlands

[5]Laboratory for Experimental Trauma Surgery, Department of Trauma Surgery, University Medical Center Regensburg, Regensburg, Germany

Correspondence
Patricia Y. W. Dankers, Institute for Complex Molecular Systems, Eindhoven University of Technology, PO Box 513, 5600 MB, Netherlands.
Email: p.y.w.dankers@tue.nl

Funding information
Dutch Polymer Institute (DPI), Grant/Award Number: 731.015.505; European Research Council (FP7/2007–2013), Grant/Award Number: 308045; Netherlands CardioVascular Research Initiative, Grant/Award Number: CVON 2012-01; The Dutch Ministry of Education, Culture and Science, Gravitation Programs, Grant/Award Numbers: 024.003.013, 024.005.020

Abstract

Antibacterial resistance against conventional antibiotics has emerged as a global health problem. To address this problem, antimicrobial peptides (AMPs) have been recognized as alternatives due to their fast-killing activity and less propensity to induce resistance. Here, the AMPs are engineered via a supramolecular fashion to control and increase their biological performance. The AMPs are modified with ureido-pyrimidinone (UPy) to obtain UPy-AMP monomers, followed by modular self-assembling to realize antibacterial UPy-AMP supramolecular polymers. These positively charged assemblies are illustrated as stable, short fibrous or rod-like UPy-AMP nanostructures with enhanced antibacterial activity and modulable cytotoxicity. Moreover, these antibacterial UPy-AMP assemblies can be internalized by both THP-1 derived macrophages and human kidney cells, which would be an effective potential therapy to deliver the AMPs into mammalian cells to address intracellular infections. Overall, the results present here demonstrate that supramolecular engineering of AMPs provides a powerful tool to enhance the antibacterial activity, modulate cytotoxicity and accelerate the clinical application of AMPs.

KEYWORDS

antibacterial biomaterials, antimicrobial peptides, bacterial infection, intracellular delivery, supramolecular nanostructures

1 | INTRODUCTION

The extensive and widespread use of conventional antibiotics has induced a rapid increase in antibacterial resistance, which has become a large global health problem.[1–6] To cope with this challenge, new antibacterial technologies and strategies including supramolecular engineered cationic surfactants[7,8] and polymers,[9–11] photosensitizer,[12,13] photothermal agents[14–16] and antibacterial peptides[3,6,17–22] are developed as alternatives. By using dynamic and reversible non-covalent interactions, engineering antibacterial materials through delicate control of supramolecular assemblies on a molecular level can be realized.[3,17,21,23–25] Moreover, this modular and tunable approach allows for incorporating functional molecules to achieve multifunctional nanostructures.[23,26–28]

Among these antibacterial supramolecular assemblies, antimicrobial peptides (AMPs)-based nanostructures has gained significant interest owing to the straightforward killing mechanism of broad-spectrum AMPs. This mechanism involves irreversible disruption of the cytoplasmic membrane of bacteria to induce cell death,[2,29,30] which exhibits low degrees of antimicrobial resistance. The currently developed supramolecular AMPs nanostructures are, however, either with compromised antibacterial activity,[18,19] or not stable under critical micelle concentration.[17] Additionally, the interactions between the engineered AMPs nanostructures and mammalian cells should be examined as understanding the fate of nanostructured AMPs and their effects on surrounding healthy tissues are critical for safe clinical applications.[31] These interactions were, unfortunately, seldom investigated.

Therefore, the current study aims to engineer the naturally derived AMPs to achieve stable nanostructures with enhanced antibacterial activity through a supramolecular fashion, as well as to investigate the interactions between the AMPs nanostructures and mammalian cells. To achieve this target, a supramolecular building block based on our four-fold hydrogen-bonding ureidopyrimidinone (UPy) unit was designed as the base monomer (UPy-OCH_3, Figure 1A). This monomer has been

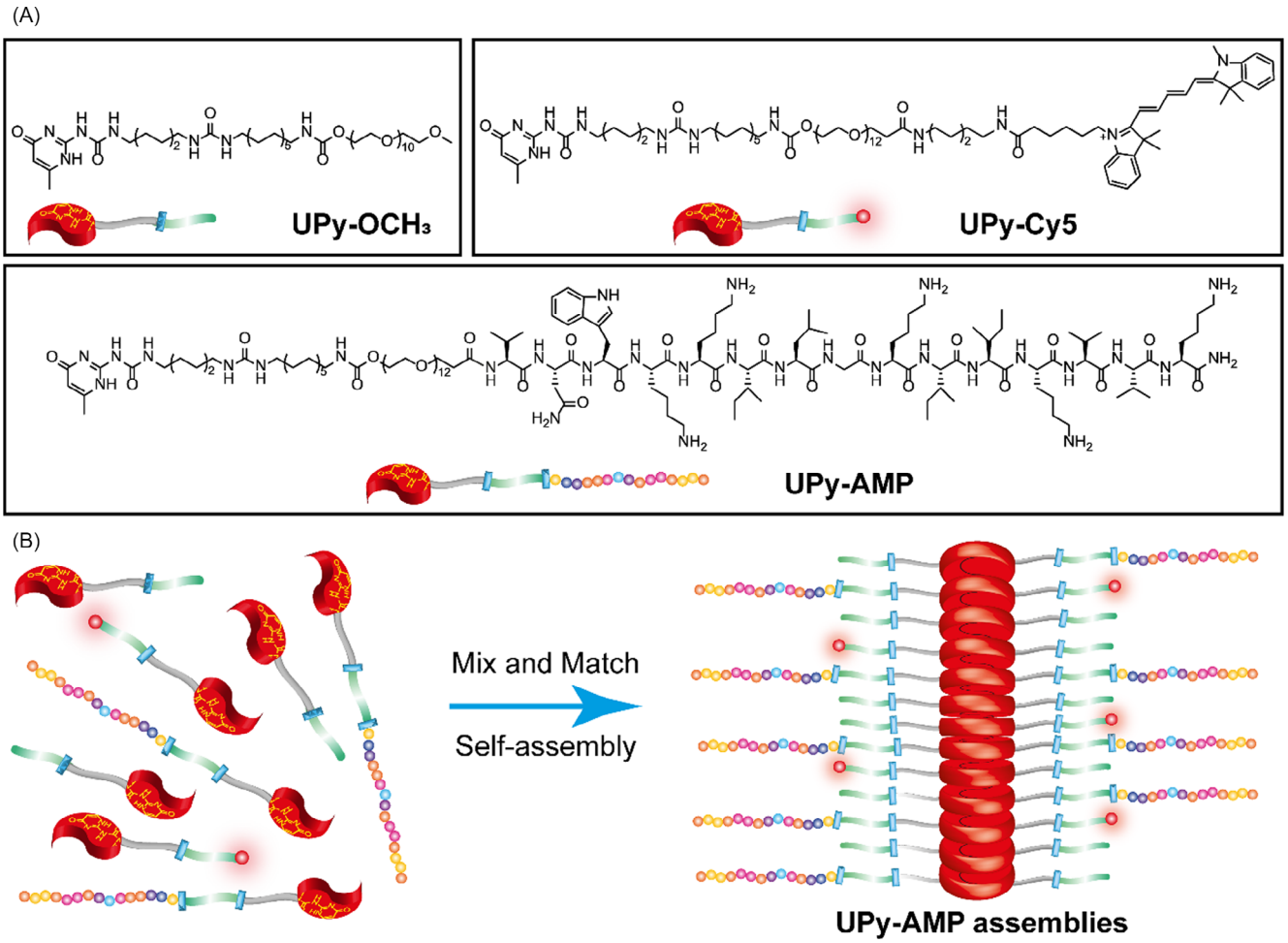

FIGURE 1 Chemical structures of UPy-monomers (A) and schematic illustration of the 1D UPy-AMP assemblies that will further aggregate into supramolecular polymer fibers (B).

demonstrated to assemble into fibrous assemblies owing to lateral stacking of hydrogen-bonded UPy-dimers, which are protected by the hydrophobic pockets formed by the alkyl spacers assisted by hydrogen-bonding of the urea groups.[26] The cationic Lasioglossin III AMP (Lasio III, VNWKKILGKIIKVVK) was selected as a model AMP in this study owing to its potent antibacterial activity against both Gram-positive and Gram-negative bacteria, low-hemolytic activity and high-cell selectivity.[22,32] It derives from the venom of the eusocial bee *Lasioglossum laticeps* and has high affinity for negatively charged pathogenic membranes.[33] This selective peptide-membrane interaction induces the Lasio III folds into an α-helix structure and lays on the surface of the membrane with its entire length, which further induces the permeabilization of the pathogenic membranes and bacteria death.[32] Besides, possible entering of Lasio III into the bacteria cell and attacking intracellular biomolecules such as nucleic acids is proposed.[32] Lasio III was conjugated to the base UPy-monomer to form the antibacterial UPy-AMP monomer (Figure 1A). To facilitate monitoring the interactions between the UPy-AMP assemblies and mammalian cells, fluorophore Cy5 was conjugated to the UPy-unit to form the UPy-Cy5 monomer (Figure 1A) as a fluorescent molecular probe. The UPy-AMP assemblies were prepared by supramolecular synthesis through a modular assembly of the various UPy-monomers in a "mix-and-match" approach[23,26,34] in phosphate buffered saline (PBS) (Figure 1B). The formed UPy-AMP assemblies were fully characterized and the biological performances of these assemblies, that is, antibacterial effects, cytocompatibility and cellular interactions with THP-1 derived macrophages and human kidney cells (HK-2), were also evaluated to promote their applications in the field of regenerative medicine.

2 | EXPERIMENTAL SECTION

2.1 | Materials

All the solvents were purchased from commercial sources and used as received, unless stated otherwise. Hoechst 33342, CellMask™ Green plasma membrane stain and Invitrogen™ Live Cell Imaging Solution were purchased from Thermo Fisher Scientific. Phorbol-12-myristate-13-acetate (PMA) was purchased from Sigma-Aldrich.

UPy-OCH_3 was synthesized as described in *Hendrikse* et al., *ChemComm*, *2017*,[28] for UPy-OCH_3 with LC–MS [M] calculated 1035.67, found 518.92 $[M + 2H]^{2+}$ and 1036.33 $[M + H]^{+}$. The LC–MS [M] of UPy-Cy5 was calculated 1701.11, found 567.75 $[M + 3H]^{3+}$, 851.06 $[M + 2H]^{2+}$ and 1701.33 $[M + H]^{+}$. The Lasio III AMP was synthesized with a solid phase peptide synthesis method as described by *Zaccaria* et al., *J. Polym. Sci. Part A: Polym. Chem.*, *2018*,[22] with LC–MS [M] calculated 1764.19, found 883.33 $[M + 2H]^{2+}$, 589.5 $[M + 3H]^{3+}$, 442.42 $[M + 4H]^{4+}$, 354.17 $[M + 5H]^{5+}$ and 295.33 $[M + 6H]^{6+}$. UPy-AMP monomer was synthesized as previously reported,[22] with LC–MS [M] calculated 2883.88, found 1442.83 $[M + 2H]^{2+}$, 962.42 $[M + 3H]^{3+}$, 722.08 $[M + 4H]^{4+}$, 577.92 $[M + 5H]^{5+}$ and 481.67 $[M + 6H]^{6+}$. The chromatogram and mass spectrum of the synthesized UPy-AMP monomer is illustrated in Figure S1.

2.2 | Preparation of UPy-AMP assemblies

UPy-OCH_3 and UPy-Cy5 were dissolved in methanol with a concentration of 2 and 0.1 mM, respectively. UPy-AMP was dissolved in methanol/water (99/1, vol/vol) containing 0.01 M HEPES solution at a concentration of 2 mM. To prepare UPy-AMP assemblies with different amounts of UPy-AMP monomers, a certain amount of UPy-monomers were mixed and injected into aqua medium, followed by equilibration at a defined time under gentle shaking at 200 rpm. For cell culture purpose, the assemblies were prepared by mixing monomer solutions and injecting them into the culture media containing 10% Fetal Bovine Serum (FBS).

2.3 | Characterizations of UPy-AMP assemblies

Formation of the UPy-AMP assemblies in PBS was examined by Nile Red (NR) encapsulation measurements as previously reported.[34] In detail, NR dissolved in methanol was added into the 50 μM UPy-AMP assemblies suspensions to reach a concentration of 5 μM, with an UPy: NR molar ratio of 10:1. The suspension was then equilibrated under shaking at 150 rpm for 5 min. The emission spectrum was recorded from 565 nm to 800 nm using an excitation wavelength of 550 nm on a Varian Cary Eclipse fluorescence spectrometer (Agilent Technologies) using Quartz cuvettes. Data from 5 scans were collected and averaged.

Encapsulation of Cy5 into the UPy-AMP assemblies was examined by fluorescence resonance energy transfer (FRET) measurements using the NR/Cy5 pair. The UPy-Cy5 was mixed with the UPy-monomers at a molar ratio of 1:100 to reach final concentrations of 0.5 μM and 50 μM, respectively. The mixtures were then injected into PBS to equilibrate for at least 3 h, followed by addition of NR with a concentration of 5 μM. After equilibrating, the emission spectrum was recorded from 540 to 800 nm

using an excitation wavelength of 520 nm on the Varian Cary Eclipse fluorescence spectrometer. Data from five scans were collected and averaged.

Zeta-potential of the UPy-AMP assemblies with a concentration of 50 μM in HEPES buffer (5 mM, pH 7.4) was measured by Laser Doppler Electrophoresis with a Malvern Zetasizer Nano-Z instrument using a folded capillary cell (DTS 1060).

Morphology of the UPy-AMP assemblies was examined by total internal reflectance fluorescence (TIRF) microscopy with a Nikon N-STORM system. The UPy-assemblies were prepared at 50 μM containing 1 mol% UPy-Cy5 in PBS and diluted to 2 μM, followed by flowing in a chamber between a glass slide and microscope coverslip (Menzel-Gläser, #1, 24 × 24 mm) which were separated by a piece of double-sided tape. The sample was annealed for 2 min and subsequently washed twice with PBS buffer. The Cy5 was excited at 647 nm and the fluorescence was filtered through a Nikon 97335 quad-band pass dichroic filter. The fluorescence was observed with a Nikon 100× objective (1.4 NA oil immersion) and the images were recorded with an EMCCD camera (ixon3, Andor with pixel size 0.165 μm).

2.4 | Cell culture

THP-1 human monocytic cells and immortalized HK-2 were purchased from ATCC and cultured at 37°C in 95% air/5% CO_2 atmosphere with Gibco™ Roswell Park Memorial Institute (RPMI) 1640 medium and Dulbecco's Modified Eagle Medium (DMEM), respectively, supplemented with 10% FBS and 1% penicillin/streptomycin (P/S). The THP-1 cells in the suspension culture were passed every other day while HK-2 cells were passed twice a week. PMA was added to the culture medium (50 ng/ml) and incubated with the monocytes for 48 h to induce differentiation of THP-1 monocytes into macrophages. For all of the cell experiments, the THP-1 cells and HK-2 cells were seeded at a density of 2.5×10^5 cells/cm^2 and 2.5×10^4 cells/cm^2, respectively.

2.5 | Cytocompatibility of UPy-AMP assemblies

The cytocompatibility of the UPy-AMP assemblies for both THP-1 derived macrophages and HK-2 cells was investigated with an LDH assay following the standard protocol (Thermo Fisher Scientific) with minor adjustments. In brief, the cells were seeded onto a 48-well plate with the above-mentioned density in triplicate. THP-1 cells were induced with PMA for 48 h and HK-2 cells were cultured overnight for attachment. Culture media containing UPy-AMP assemblies of different formulations and at various concentrations were then added into each well. The wells containing only culture medium were used as Medium control. After 24 h of incubation, lysis buffer was added into wells without UPy-AMP assemblies and incubated for 45 min at 37°C in 95% air/5% CO_2 atmosphere. These wells were used as Maximum LDH. After this, a 50 μl aliquot of cell metabolic medium of each well was transferred into a 96-well flat-bottom plate in duplicate, followed by the addition of 50 μl of the reaction mixture. The plate was then incubated at room temperature for 30 min protected from light. After incubation, 50 μl of stop solution was added to each well and the absorbance at 490 nm and 680 nm was measured with a plate reader. The LDH absorbance value was obtained by subtracting the 680-nm absorbance value (background) from the 490-nm absorbance value. The cytocompatibility of the UPy-AMP assemblies was calculated with the following equation:

$$\textit{Cytocompatibility} = 100\% - \frac{\textit{Assemblies LDH} - \textit{Medium control LDH}}{\textit{Maximum LDH} - \textit{Medium control LDH}} \times 100\%.$$

2.6 | Live/dead assay

The viability of the THP-1 derived macrophages and HK-2 cells after 24 h of incubation with certain amounts of UPy-AMP assemblies was determined by live/dead assay in way of Calcein AM and Propidium Iodide staining. In brief, THP-1 and HK-2 cells were seeded and cultured in an 8-well chamber (Thermo Scientific™ Nunc™ Lab-Tek™ with #1 borosilicate glass bottom) at a density of 2.5×10^5 cells/cm^2 and 2.5×10^4 cells/cm^2, respectively, in quadruplicate. The Calcein AM and Propidium Iodide stock solution was diluted to 10 μM in PBS. Subsequently, the cells were washed twice with PBS and 100 μl of the staining solution was added into each well. After 30 min incubation at 37°C, the cells were washed with PBS and examined by confocal laser scanning microscope (CLSM). Imaging acquisition of the cells was performed by using a Leica SP5 CLSM with a 20× objective.

2.7 | Antibacterial test of the UPy-AMP assemblies against *Staphylococcus aureus* and *Escherichia coli*

The antibacterial activities of the UPy-AMP assemblies with different compositions were evaluated against *Staphylococcus aureus* (*S. aureus*) JAR060131 and *Escherichia coli* (*E. coli*) 8735 by performing a minimal

inhibitory concentration (MIC) assay and a 99.9% lethal concentration ($LC_{99.9}$) assay in modified RPMI 1640 medium (with 20 mM HEPES and L-glutamine, without sodium bicarbonate, Sigma-Aldrich). The bacteria were cultured overnight in tryptic soy broth to mid-logarithmic growth-phase and then washed twice with PBS. After washing, the bacteria were diluted in modified RPMI-1640 medium to reach the required concentration of 10^7 colony forming units (CFU)/ml by measuring the optical density of the bacteria suspension at 620 nm, based on the established relationship between the numbers of CFU and the optical densities.

2.7.1 | MIC and $LC_{99.9}$ assay

The MIC and $LC_{99.9}$ are defined as the lowest AMP or UPy-AMP assemblies concentrations that can inhibit the visible growth of bacteria or that can kill 99.9% of bacteria after certain duration of incubating with bacteria, respectively. The MIC and $LC_{99.9}$ tests were performed according to published protocols[5,35] with minor modifications. Briefly, the pure AMP and UPy-AMP assemblies with a concentration series of 40 to 0.625 μM were prepared via a two-fold dilution method in modified RPMI 1640 medium. Ten microliter of the AMP or UPy-AMP assemblies suspension was added into a polypropylene corner notch microplate (Corning CLS3879) in quintuplet containing 80 μl RMPI. The bacteria were diluted to a concentration of 1×10^7 CFU/ml and 10 μl of bacteria suspension was added into each well to reach a final concentration of 1×10^6 CFU/ml with a final volume of 100 μl. After incubation on a shaking plate (200 rmp, 37°C) for 24 h, MIC was determined by visual assessment of bacteria growth. For the $LC_{99.9}$ at 2 h and 24 h, an aliquot of 20 μl of each incubation was taken and mixed with 20 μl of a 0.05% (vol/vol) sodium polyanethole sulfonate (SPS) solution to block the activity of the peptides. Ten microliter of this mixture was then plated on blood agar plates in duplicate. The blood agar plates were then incubated at 37°C for 24 h and the number of CFU was counted to determine the $LC_{99.9}$.

2.7.2 | Bacterial killing kinetics

To monitor the antibacterial activity of the pure AMP and UPy-AMP assemblies over time, a time-kill experiment was performed. This experiment was executed by incubating the bacteria (1.38×10^6 CFU/ml for *S. aureus* and 5.4×10^5 CFU/ml for *E. coli*) with 10 μM pure AMP or UPy-AMP assemblies of different compositions in triplicates in modified RPMI-1640 medium, in a total volume of 250 μl at 200 rpm and 37°C. At each defined time point, an aliquot of 20 μl of each incubation was taken and mixed with 20 μl of a 0.05% (vol/vol) SPS solution to stop the peptide activity. Ten microliter of this mixture was plated on blood agar plates in duplicate. The blood agar plates were incubated at 37°C for 24 h and the number of CFU was counted to determine the concentration of bacteria at different time points.

2.8 | Internalization of UPy-assemblies by mammalian cells

To monitor the interaction of UPy-AMP assemblies with the mammalian cells, the UPy-AMP assemblies (UPy-OCH_3:UPy-AMP = 25:75, 10 μM) containing 1 mol% of UPy-Cy5 as reporter were prepared in RPMI and DMEM medium containing 10% of FBS. THP-1 and HK-2 cells were seeded in an 8-well chamber (Thermo Scientific™ Nunc™ Lab-Tek™ with #1 borosilicate glass bottom) at a density of 2.5×10^5 cells/cm^2 and 2.5×10^4 cells/cm^2, respectively, in quadruplicate. After the formation of THP-1 derived macrophages and overnight attachment of HK-2 cells, the cells were washed three times with PBS and 0.4 ml of a suspension of UPy-AMP assemblies in culture medium was added in each well. At each time point, the UPy-AMP assemblies of the designated sample were washed away with PBS. The cells were sequentially stained with Hoechst 33342 and CellMask™ Green for nuclei and membranes, respectively. After staining, the cells were washed three times with PBS and Invitrogen™ Live Cell Imaging Solution was added into each well for live imaging. Live imaging was performed using a Leica SP5 CLSM at 37°C to determine the internalization of UPy-assemblies by the cells.

To examine the ability of the cells to excrete the internalized UPy-AMP assemblies, the UPy-AMP assemblies were incubated with the cells for 120 min and then washed away with PBS. Fresh medium was added to continue culture the cell for another 48 h. Subsequently, the cells were stained with Calcein AM and live confocal imaging was performed to observe the Cy5 signal from the UPy-AMP assemblies.

2.9 | Statistics

All data is depicted as average ± standard deviation. GraphPad Prism was used to do the statistical analyses. Means of experimental data were analyzed by One-way analysis of variance followed by a Tukey post hoc test. A value of $p < 0.05$ was considered as a statistically significant difference.

3 | RESULTS AND DISCUSSION

3.1 | Characterization of the UPy-AMP assemblies

The UPy-AMP assemblies were obtained by modular self-assembling of functional UPy-monomers (Figure 1A) via a "mix-and-match" fashion in PBS (Figure 1B). Specifically, the UPy-monomers were dissolved separately in methanol and a certain amount of these monomers were then thoroughly mixed. Subsequently, PBS was added into the UPy-monomers mixtures to reach a UPy-monomer concentration of 50 μM, followed by overnight equilibration on a shaking bed at 200 rpm to obtain the UPy-assemblies in aqueous environment. Five types of UPy-assemblies were prepared and the detailed formulations of these assemblies are shown in Table 1. The UPy-AMP 25 formulation, which composes 25% of UPy-AMP monomer, only formed visible clusters and agglomerated in PBS. Further experiments with this formulation were thus not carried out.

TABLE 1 Formulation of UPy-antimicrobial peptide (UPy-AMP) assemblies

Formulations	UPy-AMP: UPy-OCH_3 (molar ratio)	Note
UPy-AMP 0	0:100	—
UPy-AMP 25	25:75	Agglomerated
UPy-AMP 50	50:50	—
UPy-AMP 75	75:25	—
UPy-AMP 100	100:0	—

To evaluate the successful formation of UPy-AMP assemblies, NR was used as a probe to examine the existence of lateral hydrophobic pockets formation of the assemblies. NR prefers to partition in aggregates that contain hydrophobic domains and produces a hyperchromic effect with a blue shift.[6,36] For various formulations, strong intensity of fluorescent NR signals were observed while significant blue shift of the NR emission were not detected (Figure 2A). This absence of blue shift may be due to the presence of the high polarity of the aqueous media, which can induce a red shift of the fluorescence[37] and counteract with the blue shift generated by hydrophobic domain partition. This hyperchromic effect thus confirmed the formation of the UPy-AMP assemblies. The incorporation of UPy-Cy5 was examined by FRET with the fluorescent NR/Cy5 pair. Upon the excitation of NR as the donor, strong Cy5 signals from different formulations were detected (Figure 2B), which demonstrated that Cy5 was in close proximity with NR and the successful incorporation of UPy-Cy5 into UPy-AMP assemblies. The zeta-potential values of the assemblies

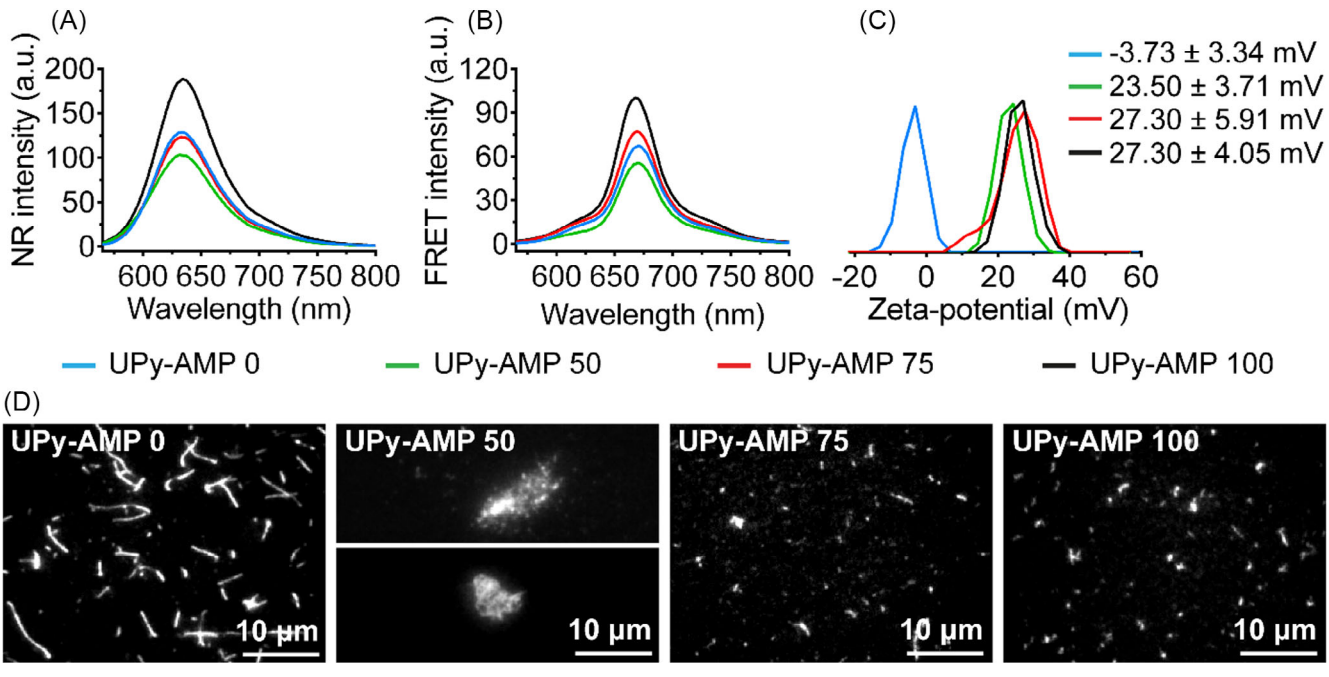

FIGURE 2 Characterization of the UPy-AMP assemblies. The formation of UPy-AMP assemblies is confirmed by intensive NR (molar ratio of UPy:NR at 10:1) signals which indicate strong hydrophobic pocket formations (A), encapsulation of UPy-Cy5 (molar ratio of UPy-Cy5:UPy-monomers at 1:100) into the UPy-AMP assemblies is confirmed by fluorescence resonance energy transfer (FRET) examination with NR/Cy5 pair (B), zeta-potentials measurements of UPy-AMP assemblies (C) and morphology of the UPy-AMP assemblies examined by TIRF microscopy with Cy5 as fluorophore (D).

measured in 5 mM HEPES buffer at pH 7.4 shifted from −3.73 ± 3.34 mV for UPy-AMP 0 to 23.50 ± 3.71, 27.30 ± 5.91 and 27.30 ± 4.05 mV for the formulations of UPy-AMP 50, 75 and 100, respectively (Figure 2C). These results indicated that the existence of UPy-AMP monomers could dramatically turn over the physicochemical properties of the assemblies due to the cationic AMPs.

The morphology of the various UPy-AMP assemblies was examined with TIRF microscopy with the assistance of UPy-Cy5 reporter. Long fibers with micrometer scale were observed for assemblies consisting of pure UPy-OCH_3 monomers (Figure 2D). With increasing the composition of UPy-AMP monomers to 50%, part of the fibrous UPy-AMP 50 assemblies aggregated into large clusters (Figure 2D). Individual and stable fibrous or rod-like structures were formed with increasing the ratio of UPy-AMP monomers to 75%, while no significant differences were observed between the UPy-AMP 75 and UPy-AMP 100 formulations (Figure 2D). These structural changes may be caused by the incorporation of UPy-AMP monomer, which would impede the polymerization process of the supramolecular system due to the charge repulsion between the positively charged groups of AMPs.[34,38]

3.2 | Antimicrobial activities of the UPy-AMP assemblies

The formation of UPy-AMP assemblies is expected to increase the local density of the positive charges and AMP mass,[17,24] which would thus enhance the antimicrobial activity of the AMPs. To test this hypothesis, the MIC and $LC_{99.9}$ of the UPy-AMP assemblies against the Gram-positive bacterium *S. aureus* and Gram-negative bacterium *E. coli* were examined. Overall, effective antibacterial properties of all the UPy-AMP assemblies against both *S. aureus* and *E. coli* were obtained (Table 2), which indicated that the original potent antibacterial activities of the AMPs were maintained after chemical functionalization with amphiphilic UPy molecules. Specifically for *E. coli*, the MIC and $LC_{99.9}$ at both 2 h and 24 h for pure AMPs and UPy-AMP 75 formulation shared the same concentration of 2.5 μM (Table 2). Identical results of the MIC and $LC_{99.9}$ at 24 h for the UPy-AMP 75 and pure AMP against *S. aureus* were also obtained, with the concentration at approximately 2.5 μM (Table 2). These results hint to a slight enhancement of their antibacterial properties as the UPy-AMP 75 formulation contained 25% less amount of active AMPs compared to the pure AMPs but achieved an identical antibacterial effect. Moreover, with increasing the ratio of UPy-AMP monomers to 100% as UPy-AMP 100 assemblies, onefold decrease of the concentrations for MIC, $LC_{99.9}$ at 2 h and 24 h can be observed compared to pure AMP (Table 2). These results demonstrate that supramolecular engineering of AMPs through UPy modification following modular self-assembling is an effective method to control the antibacterial performance of AMPs, and the antibacterial activities of the UPy-AMP assemblies depend on the amount of UPy-AMP monomer in the formulation.

As the AMPs kill bacteria with fast action,[2,29] killing kinetics of the various UPy-AMP assemblies at a concentration of 10 μM were examined in a period of 2 h to compare their activities. Although a higher $LC_{99.9}$ at 2 h was required for the UPy-AMP 75 assemblies against *S. aureus* compared to the pure AMPs formulation (Table 2), the UPy-AMP 75 assemblies killed all the *S. aureus* in 45 min when applied at the same concentration as pure AMPs (i.e., 10 μM) but effectively with 25% less amount of AMPs presented in the solution (Figure 3A). Gram-negative bacteria are generally harder to kill compared to their Gram-positive counterparts, which is largely due to the presence of an outer membrane that serves as an impermeable barrier.[3,39,40] For *E. coli*, the UPy-AMP 75 assemblies achieved even better killing kinetics compared to the pure AMPs (Figure 3B), which again demonstrated the enhancement of the antibacterial activity of AMP through supramolecular engineering.[17]

3.3 | Cytocompatibility of the UPy-AMP assemblies

Although AMPs are promising antibacterial agents, their potential cytotoxicity towards mammalian cells,

TABLE 2 MIC and $LC_{99.9}$ of pure AMP and UPy-AMP assemblies

	S. aureus (μM)			*E. coli* (μM)		
Formulations	**$LC_{99.9}$, 2 h**	**MIC**	**$LC_{99.9}$, 24 h**	**$LC_{99.9}$, 2 h**	**MIC**	**$LC_{99.9}$, 24 h**
Pure AMP	2.5	2.5	2.5	2.5	2.5	2.5
UPy-AMP 50	>40	5	10–20	5	5	5
UPy-AMP 75	10	2.5	2.5–5	2.5	2.5	2.5
UPy-AMP 100	5	1.25	2.5–5	1.25	1.25	1.25

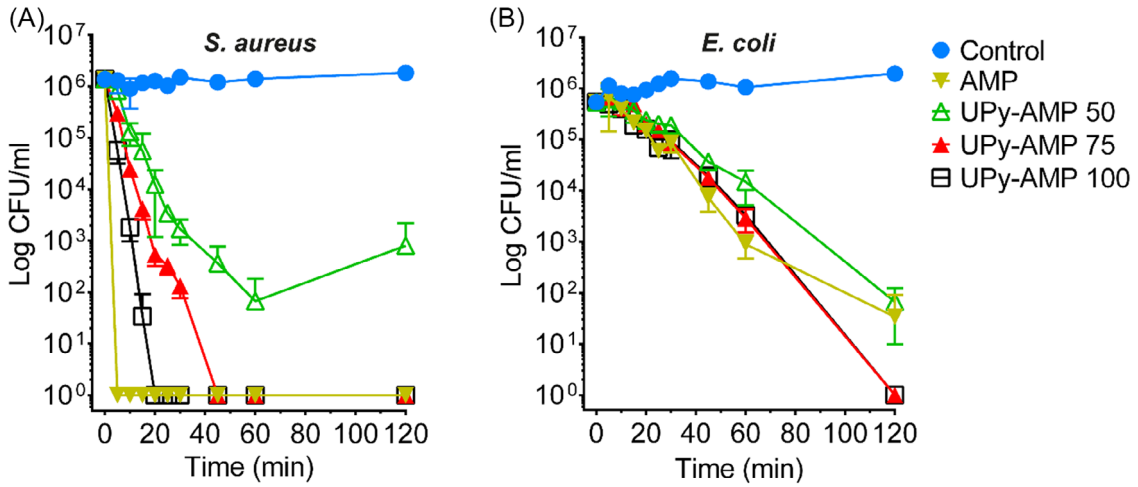

FIGURE 3 Antibacterial effects of the UPy-AMP assemblies in term of time-killing on *S. aureus* (A) and *E. coli* (B) in 120 min. The concentrations of the pure AMP and UPy-AMP assemblies were 10 μM.

which originates from their cationic nature, limited their success in clinical settings.[2,3,41] Therefore, the cytocompatibility of the UPy-AMP assemblies should be examined to receive the biocompatible concentration range for safe clinical applications. To achieve this, the UPy-AMP assemblies with different formulations and at various concentrations was quantitatively and qualitatively investigated with an LDH method and live/dead staining examination for both THP-1 derived macrophages and HK-2 cells. The cell culture medium without the addition of any UPy-AMP assemblies was used as the positive control.

The cytocompatibility of the UPy-AMP assemblies for both types of cells was dependent on the concentrations and compositions of the UPy-AMP assemblies (Figure 4A,B). All of the UPy-AMP assemblies did not show a cytotoxic effect at the concentration of 5 μM according to the ISO 10993-5:2009 standard, which indicates 30% reduction of cell viability as toxic (Figure 4A,B). With increasing the concentration to 10 μM, only UPy-AMP 100 became significantly cytotoxic (Figure 4A,B). At the concentration of 20 μM, all of the UPy-AMP assemblies induced significant cytotoxicity and the toxic level was positively correlated with the amount of UPy-AMP monomers. An identical trend was observed from the results of the live/dead viability examinations (Figure 4C,D). These results demonstrated that the cytocompatibility of the UPy-AMP assemblies could be easily adjusted through modular supramolecular engineering.

3.4 | Biological interactions between the UPy-AMP assemblies and mammalian cells

Considering the safe clinical application of the UPy-AMP assemblies, the fate of these antibacterial nanostructures and their influence on mammalian cells should be examined. When these antibacterial assemblies are administrated, they will confront cleaning by a mononuclear phagocyte system which is mainly composed of resident macrophages.[42] Moreover, these nanostructures may actively interact with non-phagocytic cells due to their relatively small size.[43] Therefore, the interactions between the UPy-AMP assemblies and phagocytic cells, that is, THP-1 derived macrophages and non-phagocytic cells, that is, HK-2 cells were examined. The UPy-AMP 75 assemblies at the concentration of 10 μM were chosen for material-cell interaction experiments due to their excellent cytocompatibility and antibacterial activity. After different time periods of incubation with the cells, the extracellular UPy-AMP 75 assemblies were washed away with PBS to stop their continued internalization by cells. The cells were then stained and observed by CLSM to determine the internalization of UPy-assemblies by the cells.

These UPy-AMP assemblies could be internalized by both types of cells within 30 min (Figure 5). With increasing the incubation time to 120 min, more of the assemblies were internalized. These results indicated that the AMPs could be easily transferred into the mammalian cells after being supramolecular engineered into nanostructures. This exciting phenomenon provides a promising potential therapy for the treatment of intracellular infections, where the bacteria can survive and persist both inside macrophages[44,45] and non-professional phagocytes, that is, endothelial or epithelial cells and osteoblast.[46] Although therapies involving intracellular delivery of AMPs have been developed,[46,47] these therapies required complicated carrier design and target only one type of cell. In contrast, the supramolecular engineered UPy-AMP assemblies have the potential to target the intracellular bacteria inside several types of cells.

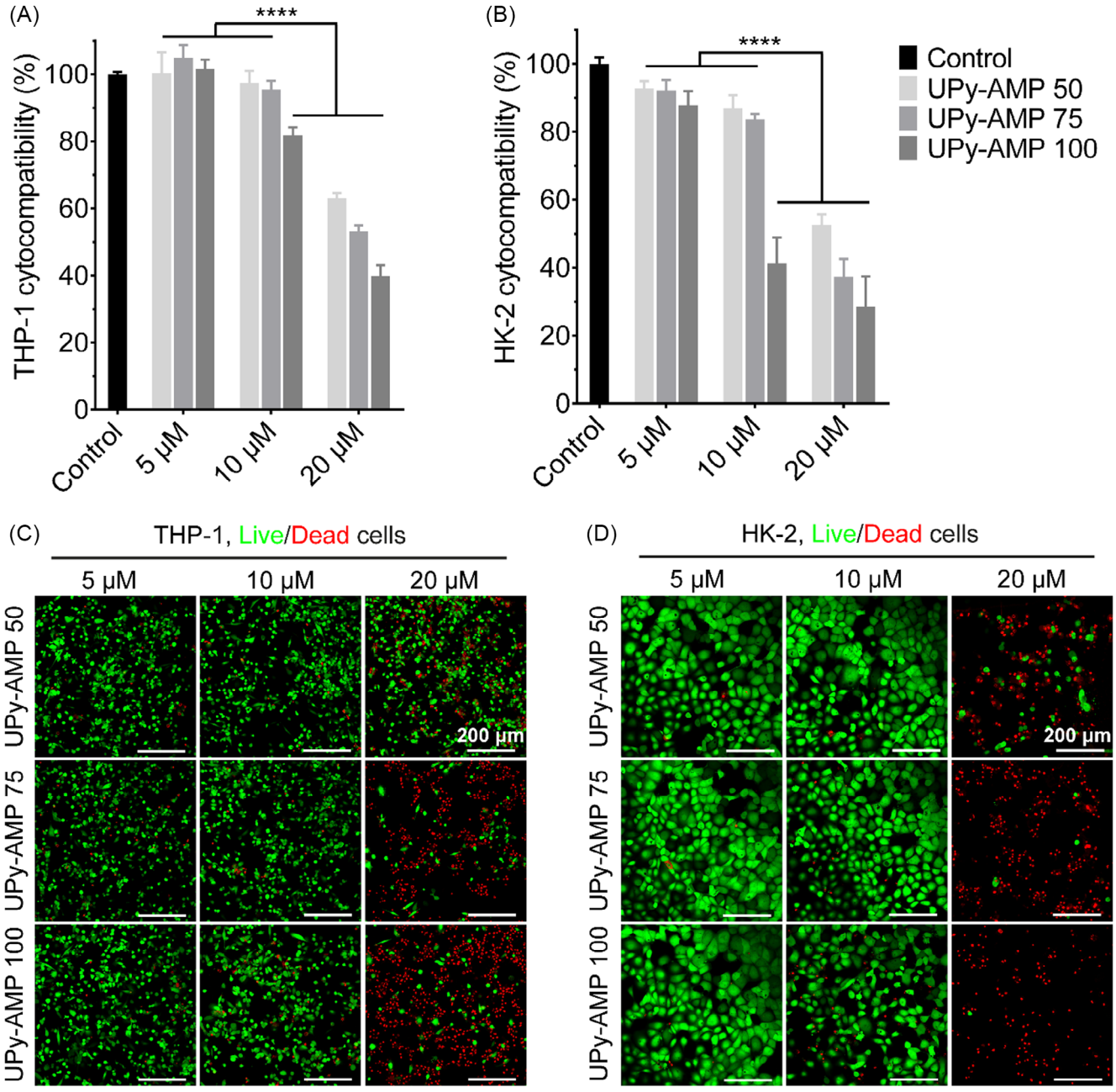

FIGURE 4 Biological examinations of the UPy-AMP assemblies with THP-1 derived macrophages (A and C) and HK-2 cells (B and D) by means of cytocompatibility (A and B) and live/dead staining (C and D). Scale bars represent 200 μm in C and D. $p < 0.0001$ (****).

Additionally, with increasing the incubation time to 24 and 48 h, the cells internalized more of the UPy-AMP assemblies and maintained good viability (Figure S2a and Figure S3a). These results confirmed the long-term cytocompatibility of these UPy-AMP assemblies.

To achieve clinical translation of these UPy-AMP assemblies, they should function as a drug that can be easily cleared from the body after executing their tasks. After 120 min incubation of the UPy-AMP assemblies with the mammalian cells, fibrous structures from the Cy5 signal were observed inside both types of cells (Figure 5 zoomed in area), which indicated the possible attachment of the UPy-AMP assemblies to mitochondria (unpublished data). The extracellular UPy-AMP assemblies were then washed away and the cells were continuously incubated for another 48 h to determine the excretion of the UPy-AMP assemblies by cells. A dramatic decrease of the Cy5 signal was observed for both types of cells (Figure 5) and the cells maintained good viability (Figure S2b and S3b). These results suggested that the internalized UPy-AMP assemblies could be excreted by mammalian cells while did not harm the

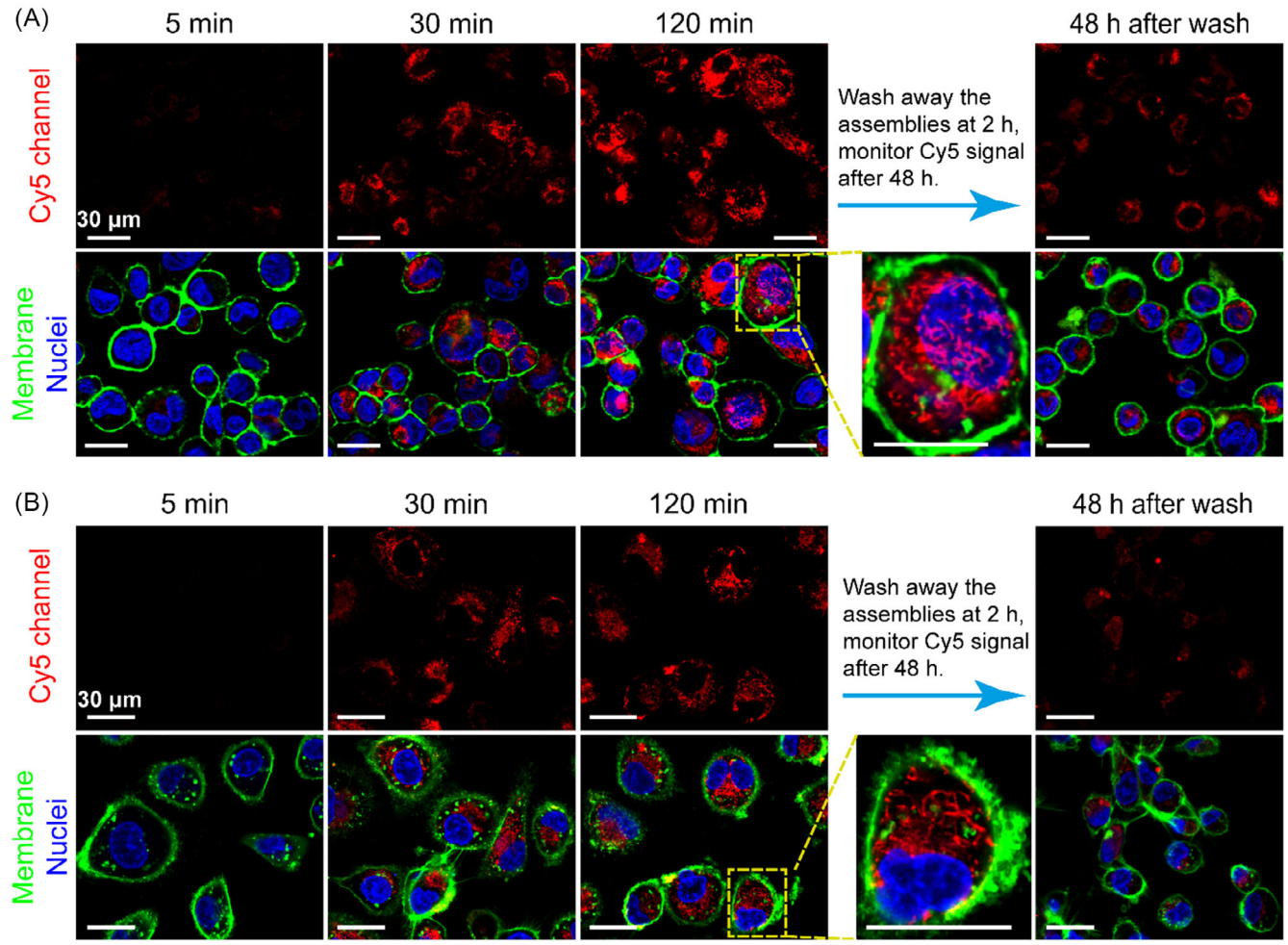

FIGURE 5 Confocal fluorescent micrographs of the internalization of the UPy-AMP 75 assemblies (10 μM) by THP-1 derived macrophages (A) and HK-2 cells (B). The UPy-AMP 75 assemblies were labeled with Cy5 (red), nuclei and membranes of the cells were stained blue and green, respectively. Scale bars represent 30 μm.

viability of the cells, which strongly supports their safe clinical applications for the treatment of infections or used as antibacterial biomaterials.

All the above results demonstrate the proof-of-concept of supramolecular engineering the Lasio III AMP to form the stable UPy-AMP assemblies with enhanced antibacterial activity. Despite this promising advantage, these UPy-AMP assemblies confront complex biological barriers upon systemic or local administration. These barriers include possible protease degradation[48] and potential side interactions with various serum proteins.[49] Although formation of supramolecular AMP assemblies can improve the protease susceptibilities of AMP,[6] the integrity of the UPy-AMP monomer and antibacterial activity of the UPy-AMP assemblies against protease degradation can be further investigated to optimize their therapeutic concentrations. Besides, systemic investigation of the (dynamic) stability of these UPy-AMP assemblies under different conditions, for example, dilution and the presence of a variety of serum proteins, would be beneficial for clinical application of these UPy-AMP assemblies.

4 | CONCLUSION

In conclusion, stable supramolecular antibacterial assemblies were successfully fabricated through supramolecular engineering of the natural derived AMP with UPy molecules. These antibacterial UPy-AMP assemblies demonstrated improved performance of antibacterial activity against both Gram-positive *S. aureus* and Gram-negative *E. coli* with good cytocompatibility. These UPy-AMP assemblies could be internalized by both THP-1 derived macrophages and HK-2 cells for intracellular delivery of AMP. And the internalized UPy-AMP assemblies could be excreted by the mammalian cells after 48 h. These properties endowed the UPy-AMP assemblies

as promising antibacterial biomaterials for regenerative medicine.

ACKNOWLEDGMENTS

This work was supported by the Netherlands Cardiovascular Research Initiative (CVON 2012-01), the European Research Council (FP7/2007–2013) ERC Grant Agreement 308045, the Dutch Polymer Institute (DPI) project 731.015.505, and the Dutch Ministry of Education, Culture and Science (Gravity programs 024.003.013 and 024.005.020).

CONFLICT OF INTEREST STATEMENT

The authors declare no conflict of interest.

DATA AVAILABILITY STATEMENT

The data that support the findings of this study are available from the corresponding author upon reasonable request.

ORCID

Patricia Y. W. Dankers https://orcid.org/0000-0002-8997-181X

REFERENCES

[1] G. L. French, *Adv. Drug Deliv. Rev.* **2005**, *57*, 1514.
[2] R. E. Hancock, H. G. Sahl, *Nat. Biotechnol.* **2006**, *24*, 1551.
[3] S. J. Lam, N. M. O'Brien-Simpson, N. Pantarat, A. Sulistio, E. H. H. Wong, Y.-Y. Chen, J. C. Lenzo, J. A. Holden, A. Blencowe, E. C. Reynolds, G. G. Qiao, *Nat. Microbiol.* **2016**, *1*, 16162.
[4] R. Nordström, M. Malmsten, *Adv. Colloid Interface Sci.* **2017**, *242*, 17.
[5] A. de Breij, M. Riool, R. A. Cordfunke, N. Malanovic, L. de Boer, R. I. Koning, E. Ravensbergen, M. Franken, T. van der Heijde, B. K. Boekema, P. H. S. Kwakman, N. Kamp, A. El Ghalbzouri, K. Lohner, S. A. J. Zaat, J. W. Drijfhout, P. H. Nibbering, *Sci. Trans. Med.* **2018**, *10*, eaan4044.
[6] L. Lombardi, Y. Shi, A. Falanga, E. Galdiero, E. de Alteriis, G. Franci, I. Chourpa, H. S. Azevedo, S. Galdiero, *Biomacromolecules* **2019**, *20*, 1362.
[7] C. Zhou, D. Wang, M. Cao, Y. Chen, Z. Liu, C. Wu, H. Xu, S. Wang, Y. Wang, *ACS Appl. Mater. Interfaces* **2016**, *8*, 30811.
[8] Y. Shen, S. Li, R. Qi, C. Wu, M. Yang, J. Wang, Z. Cai, K. Liu, J. Yue, B. Guan, Y. Han, S. Wang, Y. Wang, *Angew. Chem. Int. Ed.* **2022**, *61*, e202110938.
[9] L. D. de Melo Carrasco, J. L. M. Sampaio, A. M. Carmona-Ribeiro, *Int. J. Mol. Sci.* **2015**, *16*, 6337.
[10] L. Wang, Q. Zhao, Z. Zhang, Z. Lu, Y. Zhao, Y. Tang, *ACS Appl. Bio Mater.* **2018**, *1*, 1478.
[11] S. Yan, S. Chen, X. Gou, J. Yang, J. An, X. Jin, Y.-W. Yang, L. Chen, H. Gao, *Adv. Funct. Mater.* **2019**, *29*, 1904683.
[12] L. Chen, H. Bai, J.-F. Xu, S. Wang, X. Zhang, *ACS Appl. Mater. Interfaces* **2017**, *9*, 13950.
[13] E. Lee, X. Li, J. Oh, N. Kwon, G. Kim, D. Kim, J. Yoon, *Chem. Sci.* **2020**, *11*, 5735.
[14] Y. Yang, P. He, Y. Wang, H. Bai, S. Wang, J.-F. Xu, X. Zhang, *Angew. Chem. Int. Ed.* **2017**, *56*, 16239.
[15] S. Tian, H. Bai, S. Li, Y. Xiao, X. Cui, X. Li, J. Tan, Z. Huang, D. Shen, W. Liu, P. Wang, B. Z. Tang, C.-S. Lee, *Angew. Chem. Int. Ed.* **2021**, *60*, 11758.
[16] Z. Yin, Y. Yang, J. Yang, G. Song, H. Hu, P. Zheng, J.-F. Xu, *CCS Chem.* **2022**, *4*, 3285.
[17] L. Liu, K. Xu, H. Wang, P. K. Jeremy Tan, W. Fan, S. S. Venkatraman, L. Li, Y.-Y. Yang, *Nat. Nanotechnol.* **2009**, *4*, 457.
[18] Y. Liu, Y. Yang, C. Wang, X. Zhao, *Nanoscale* **2013**, *5*, 6413.
[19] D. Xu, L. Jiang, A. Singh, D. Dustin, M. Yang, L. Liu, R. Lund, T. J. Sellati, H. Dong, *Chem. Commun.* **2015**, *51*, 1289.
[20] M. Beter, H. K. Kara, A. E. Topal, A. Dana, A. B. Tekinay, M. O. Guler, *Mol. Pharm.* **2017**, *14*, 3660.
[21] B. Hu, C. Owh, P. L. Chee, W. R. Leow, X. Liu, Y.-L. Wu, P. Guo, X. J. Loh, X. Chen, *Chem. Soc. Rev.* **2018**, *47*, 6917.
[22] S. Zaccaria, R. C. van Gaal, M. Riool, S. A. J. Zaat, P. Y. W. Dankers, *J. Polym. Sci., Part A: Polym. Chem.* **2018**, *56*, 1926.
[23] M. J. Webber, R. Langer, *Chem. Soc. Rev.* **2017**, *46*, 6600.
[24] X. Li, H. Bai, Y. Yang, J. Yoon, S. Wang, X. Zhang, *Adv. Mater.* **2019**, *31*, 1805092.
[25] S. Guo, Y. He, Y. Zhu, Y. Tang, B. Yu, *Pharmaceuticals* **2022**, *15*, 804.
[26] M. H. Bakker, C. C. Lee, E. W. Meijer, P. Y. Dankers, L. Albertazzi, *ACS Nano* **1845**, *2016*, 10.
[27] O. J. G. M. Goor, S. I. S. Hendrikse, P. Y. W. Dankers, E. W. Meijer, *Chem. Soc. Rev.* **2017**, *46*, 6621.
[28] S. I. S. Hendrikse, S. P. W. Wijnands, R. P. M. Lafleur, M. J. Pouderoijen, H. M. Janssen, P. Y. W. Dankers, E. W. Meijer, *Chem. Commun.* **2017**, *53*, 2279.
[29] M. Zasloff, *Nature* **2002**, *415*, 389.
[30] H. Moravej, Z. Moravej, M. Yazdanparast, M. Heiat, A. Mirhosseini, M. Moosazadeh Moghaddam, R. Mirnejad, *Microb. Drug Resist.* **2018**, *24*, 747.
[31] B. Pelaz, C. Alexiou, R. A. Alvarez-Puebla, F. Alves, A. M. Andrews, S. Ashraf, L. P. Balogh, L. Ballerini, A. Bestetti, C. Brendel, S. Bosi, M. Carril, W. C. W. Chan, C. Chen, X. Chen, X. Chen, Z. Cheng, D. Cui, J. Du, C. Dullin, A. Escudero, N. Feliu, M. Gao, M. George, Y. Gogotsi, A. Grünweller, Z. Gu, N. J. Halas, N. Hampp, R. K. Hartmann, M. C. Hersam, P. Hunziker, J. Jian, X. Jiang, P. Jungebluth, P. Kadhiresan, K. Kataoka, A. Khademhosseini, J. Kopeček, N. A. Kotov, H. F. Krug, D. S. Lee, C.-M. Lehr, K. W. Leong, X.-J. Liang, M. L. Lim, L. M. Liz-Marzán, X. Ma, P. Macchiarini, H. Meng, H. Möhwald, P. Mulvaney, A. E. Nel, S. Nie, P. Nordlander, T. Okano, J. Oliveira, T. H. Park, R. M. Penner, M. Prato, V. Puntes, V. M. Rotello, A. Samarakoon, R. E. Schaak, Y. Shen, S. Sjöqvist, A. G. Skirtach, M. G. Soliman, M. M. Stevens, H.-W. Sung, B. Z. Tang, R. Tietze, B. N. Udugama, J. S. VanEpps, T. Weil, P. S. Weiss, I. Willner, Y. Wu, L. Yang, Z. Yue, Q. Zhang, Q. Zhang, X.-E. Zhang, Y. Zhao, X. Zhou, W. J. Parak, *ACS Nano.* **2017**, *11*, 2313.
[32] F. Battista, R. Oliva, P. del Vecchio, R. Winter, L. Petraccone, *Int. J. Mol. Sci.* **2021**, *22*, 2857.
[33] V. Cerovsky, M. Budesinsky, O. Hovorka, J. Cvacka, Z. Voburka, J. Slaninova, L. Borovickova, V. Fucik, L.

Bednarova, I. Votruba, J. Straka, *ChemBioChem* **2009**, *10*, 2089.
[34] M. H. Bakker, R. E. Kieltyka, L. Albertazzi, P. Y. W. Dankers, *RSC Adv.* **2016**, *6*, 110600.
[35] I. Wiegand, K. Hilpert, R. E. W. Hancock, *Nat. Protoc.* **2008**, *3*, 163.
[36] P. Greenspan, S. D. Fowler, *J. Lipid Res.* **1985**, *26*, 781.
[37] D. L. Sackett, J. Wolff, *Anal. Biochem.* **1987**, *167*, 228.
[38] P. Besenius, G. Portale, P. H. H. Bomans, H. M. Janssen, A. R. A. Palmans, E. W. Meijer, *Proc. Natl. Acad. Sci. U. S. A.* **2010**, *107*, 17888.
[39] G. Taubes, *Science* **2008**, *321*, 356.
[40] S. Gruenheid, H. Le Moual, *FEMS Microbiol. Lett.* **2012**, *330*, 81.
[41] F. Nederberg, Y. Zhang, J. P. K. Tan, K. Xu, H. Wang, C. Yang, S. Gao, X. D. Guo, K. Fukushima, L. Li, J. L. Hedrick, Y.-Y. Yang, *Nat. Chem.* **2011**, *3*, 409.
[42] D. E. Owens, N. A. Peppas, *Int. J. Pharm.* **2006**, *307*, 93.
[43] R. A. Petros, J. M. DeSimone, *Nat. Rev. Drug Discov.* **2010**, *9*, 615.
[44] S. M. Lehar, T. Pillow, M. Xu, L. Staben, K. K. Kajihara, R. Vandlen, L. DePalatis, H. Raab, W. L. Hazenbos, J. H. Morisaki, J. Kim, S. Park, M. Darwish, B. C. Lee, H. Hernandez, K. M. Loyet, P. Lupardus, R. Fong, D. Yan, C. Chalouni, E. Luis, Y. Khalfin, E. Plise, J. Cheong, J. P. Lyssikatos, M. Strandh, K. Koefoed, P. S. Andersen, J. A. Flygare, M. Wah Tan, E. J. Brown, S. Mariathasan, *Nature* **2015**, *527*, 323.
[45] Z. Yang, J. Zheng, C.-F. Chan, I. L. K. Wong, B. S. Heater, L. M. C. Chow, M. M. M. Lee, M. K. Chan, *Biomaterials* **2019**, *217*, 119286.
[46] B. Löffler, L. Tuchscherr, S. Niemann, G. Peters, *Int. J. Med. Microbiol.* **2014**, *304*, 170.
[47] J. H. Yeom, B. Lee, D. Kim, J. K. Lee, S. Kim, J. Bae, Y. Park, K. Lee, *Biomaterials* **2016**, *104*, 43.
[48] A. Rai, R. Ferrão, P. Palma, T. Patricio, P. Parreira, E. Anes, C. Tonda-Turo, M. C. L. Martins, N. Alves, L. Ferreira, *J. Mater. Chem. B* **2022**, *10*, 2384.
[49] E. Fuentes, Y. Gabaldón, M. Collado, S. Dhiman, J. A. Berrocal, S. Pujals, L. Albertazzi, *J. Am. Chem. Soc.* **2022**, *144*, 21196.

SUPPORTING INFORMATION

Additional supporting information can be found online in the Supporting Information section at the end of this article.

How to cite this article: J. Song, M. G. J. Schmitz, M. Riool, S. Guo, S. A. J. Zaat, P. Y. W. Dankers, *J. Polym. Sci.* **2023**, 1. https://doi.org/10.1002/pol.20230282